

# Conjugal transfer and mobilization capacity of the completely sequenced naphthalene plasmid pNAH20 from multiplasmid strain *Pseudomonas fluorescens* PC20

Eeva Heinaru, Eve Vedler, Jekaterina Jutkina, Merit Aava & Ain Heinaru

Institute of Molecular and Cell Biology, Tartu University, Tartu, Estonia

**Correspondence:** Eve Vedler, Institute of Molecular and Cell Biology, Tartu University, 23 Riia street, 51010 Tartu, Estonia. Tel.: +372 737 5014; fax: +372 742 0286; e-mail: eve.vedler@ut.ee

Received 4 May 2009; revised 28 July 2009; accepted 29 July 2009.  
Final version published online 10 September 2009.

DOI:10.1111/j.1574-6941.2009.00763.x

Editor: Kornelia Smalla

## Keywords

*Pseudomonas fluorescens* PC20; naphthalene and phenol plasmids; plasmid transfer; plasmid mobilization; IS elements.

## Abstract

The complete 83 042-bp nucleotide sequence of the IncP-9 naphthalene degradation plasmid pNAH20 from *Pseudomonas fluorescens* PC20 exhibits striking similarity in size and sequence to another naphthalene (NAH) plasmid pDTG1. However, the positions of insertion sequence (IS) elements significantly alter both catabolic and backbone functions provided by the two plasmids. In pDTG1, insertion of a pCAR1 ISPre1-like element disrupts expression of the lower naphthalene operon and this strain utilizes the chromosomal pathway for complete naphthalene degradation. In pNAH20, this operon is intact and functional. The transfer frequency of pNAH20 is 100 times higher than that of pDTG1 probably due to insertion of the pCAR1 ISPre2-like element into the *mpfR* gene coding for a putative repressor of the *mpf* operon responsible for mating pilus formation. We also demonstrate *in situ* plasmid transfer – we isolated a rhizosphere transconjugant strain of pNAH20, *P. fluorescens* NS8. The plasmid pNS8, a derivative of pNAH20, lacks the ability to self-transfer as a result of an additional insertion event of ISPre2-like element that disrupts the gene coding for VirB2-like major pilus protein MpfA. The characteristics of the strain PC20 and the conjugal transfer/mobilization capacity of pNAH20 (or its backbone) make this strain/plasmid a potentially successful tool for bioremediation applications.

## Introduction

Catabolic plasmids containing biodegradative genes play an important role in the degradation of (poly)aromatic compounds. The growth on phenol (PHE) is by virtue of plasmid-encoded multi- or single-component phenol hydroxylases (PH) via catechol 2,3- (C23O) or catechol 1,2-dioxygenase (C12O), respectively (Kivisaar *et al.*, 1989; Shingler *et al.*, 1989). Although the discovery, biochemistry and genetics of the degradation pathways encoded by PHE plasmids have been investigated by many researchers, their complete sequences are not available. Many plasmids responsible for degradation of polyaromatic compounds have been reported and only four naphthalene (NAH) plasmids have been entirely sequenced. The first entirely sequenced catabolic plasmid pNL1 from *Novosphingobium* (formerly *Sphingomonas*) *aromaticivorans* F199 carries the genes for the degradation of naphthalene, toluene, xylene and biphenyl

(Romine *et al.*, 1999). The other sequenced naphthalene plasmids from *Pseudomonas putida* are pDTG1, pND6-1 and NAH7 (Dennis & Zylstra, 2004; Li *et al.*, 2004; Sota *et al.*, 2006). Aerobic degradation of polyaromatic compounds proceeds through a dioxygenase attack on an aromatic ring, resulting in formation of *cis*-dihydrodiol (Cerniglia, 1992; Eaton & Chapman, 1992). The intermediate salicylate, formed after rearomatization reactions, is further catabolized via catechol or gentisate by C23O or C12O and gentisate 1,2-dioxygenase, respectively.

Bacterial conjugation is a unique process that allows the transfer of plasmid DNA from a donor to a recipient, with cell-to-cell contact being one of the most widespread mechanisms for horizontal DNA transfer with potential for universal DNA delivery (Llosa & de la Cruz, 2005). The transfer of catabolic plasmids between bacterial strains increases functional diversity and indicates the biodegradative potential of a polluted environment. Transmissible

broad-host-range plasmids are the major vehicles of horizontal gene transfer (HGT), being the basis for their evolutionary success (Heuer *et al.*, 2008). Transmissible plasmids can be classified according to their mobilization activity, as being conjugative (self-transmissible, encoding a full set of conjugative transfer genes) or mobilizable (transmissible only if a functional conjugative apparatus is provided by a conjugative plasmid present in the same host cell) (Francia *et al.*, 2004). Mobilizable plasmids usually carry a mobilization region (*mob*) encoding specific relaxosome components and the origin of transfer (*oriT*).

This study focuses on the characterization of a multi-plasmid system of *Pseudomonas fluorescens* biotype F strain PC20 isolated from river water continuously polluted by phenolic leachate (Heinaru *et al.*, 2000; Merimaa *et al.*,

2006). The transferability (both during bioaugmentation experiments and under laboratory conditions), plasmid-mobilizing capacity and the whole sequence of one plasmid of PC20 are determined. The strain PC20 is the dominant degrader in oil-amended microcosms (Heinaru *et al.*, 2005) and it was shown to survive at least > 1 year in a field bioaugmentation experiment (Juhanson *et al.*, 2009).

## Materials and methods

### Bacterial strains, plasmids and culture conditions

The bacterial strains and plasmids used in this study are listed in Table 1. The *P. fluorescens* strains PC20, 8R2ACX

**Table 1.** Bacterial strains and plasmids used in this study

Bacterial strain	Relevant phenotype*	Source or reference
<i>P. fluorescens</i> strains		
PC20	Wild-type strain harbouring pNAH20 and pPHE20, Phe <sup>+</sup> Sal <sup>+</sup> Nah <sup>+</sup>	Heinaru <i>et al.</i> (2000); this study
8R2ACX	Wild-type strain, Phe <sup>-</sup> Sal <sup>-</sup> Nah <sup>-</sup>	This study
8R2ACX (pNAH20)	Wild-type strain harbouring pNAH20, Phe <sup>-</sup> Sal <sup>+</sup> Nah <sup>+</sup>	This study
8R2ACX (pPHE20)	Wild-type strain harbouring pPHE20, Phe <sup>+</sup> Sal <sup>-</sup> Nah <sup>-</sup>	This study
NS8	Wild-type strain harbouring pNS8, Phe <sup>-</sup> Sal <sup>+</sup> Nah <sup>+</sup>	This study
<i>P. putida</i> strains		
PaW340	Phe <sup>-</sup> Sal <sup>-</sup> Nah <sup>-</sup> Sm <sup>r</sup> Trp <sup>-</sup>	Franklin & Williams (1980)
PaW340 (pNAH20)	PaW340 derivative harbouring pNAH20, Phe <sup>-</sup> Sal <sup>+</sup> Nah <sup>+</sup> Sm <sup>r</sup> Trp <sup>-</sup>	This study
PaW340 (pPHE20)	PaW340 derivative harbouring pPHE20, Phe <sup>+</sup> Sal <sup>-</sup> Nah <sup>-</sup> Sm <sup>r</sup> Trp <sup>-</sup>	This study
PaW340 (pNAH20, pPHE20)	PaW340pPHE20 derivative harbouring pNAH20, Phe <sup>+</sup> Sal <sup>+</sup> Nah <sup>+</sup> Sm <sup>r</sup> Trp <sup>-</sup>	This study
PaW340 (pDTG1, pPHE20)	PaW340pPHE20 derivative harbouring pDTG1, Phe <sup>+</sup> Sal <sup>+</sup> Nah <sup>+</sup> Sm <sup>r</sup> Trp <sup>-</sup>	This study
PaW340 (NAH7, pPHE20)	PaW340pPHE20 derivative harbouring NAH7, Phe <sup>+</sup> Sal <sup>+</sup> Nah <sup>+</sup> Sm <sup>r</sup> Trp <sup>-</sup>	This study
PaW85	Phe <sup>-</sup> Sal <sup>-</sup> Nah <sup>-</sup>	Bayley <i>et al.</i> (1977)
PaW85 (pNAH20)	PaW85 derivative harbouring pNAH20, Phe <sup>-</sup> Sal <sup>+</sup> Nah <sup>+</sup>	This study
PaW85 (pPHE20)	PaW85 derivative harbouring pPHE20, Phe <sup>-</sup> Sal <sup>+</sup> Nah <sup>+</sup>	This study
EST1412	PaW85 carrying pEST1412, Phe <sup>+</sup> Cb <sup>r</sup>	Kivisaar <i>et al.</i> (1990)
PaW85 <i>recA::tet</i>	PaW85 <i>recA</i> defective derivative	Tegova <i>et al.</i> (2004)
NCIB 9816-4	Wild-type strain harbouring pDTG1, Sal <sup>+</sup> Nah <sup>+</sup>	Serdar & Gibson (1989); Stuart-Keil <i>et al.</i> (1998)
G7	Wild-type strain harbouring NAH7 plasmid, Sal <sup>+</sup> Nah <sup>+</sup>	Dunn & Gunsalus (1973)
<i>E. coli</i> strain		
HB101 (pRK2013)	HB101 harbouring pRK2013, Km <sup>r</sup>	Boyer & Roulland-Dussoix (1969); Figurski & Helinski (1979)

\*Sm<sup>r</sup>, resistance to streptomycin; Cb<sup>r</sup>, resistance to carbenicillin; Km<sup>r</sup>, resistance to kanamycin; Phe<sup>+</sup>, Sal<sup>+</sup>, Nah<sup>+</sup>, the ability to degrade phenol, salicylic acid and naphthalene, respectively; Trp<sup>-</sup>, requirement for tryptophan in the growth medium.

and NS8 were all isolated in the northeastern part of Estonia – the two latter strains from a birch rhizosphere in phytoremediation test plots in a semi-coke (oil shale chemical industry solid waste) depository, and PC20 from the river water near the semi-coke depository.

*Pseudomonas* cells were grown in liquid or solid minimal media (MM) supplied with filter-sterilized substrates (Heinaru *et al.*, 2000). Final concentrations of substrates in medium were 2.5 mM phenol or 5 mM salicylic acid. Growth on naphthalene was studied in naphthalene vapours. Liquid cultures were grown at 30 °C on a rotary shaker.

### Methods for DNA manipulations

Bacterial genomic DNA was prepared using UltraClean microbial DNA isolation kit (Mo Bio Laboratories, Solana Beach, CA) according to the manufacturer's instructions. Plasmid DNA was isolated using the procedures of Connors & Barnsley (1982). PCR was performed with *Taq* polymerase (MBI Fermentas) and the primers used, together with annealing temperatures and sizes of the expected PCR products, are listed in Table 2. All other PCR conditions used in this study have been described previously (Heinaru *et al.*, 2005; Merimaa *et al.*, 2006). Southern blotting was performed according to standard protocols (Sambrook *et al.*, 1989). The blot was hybridized with radioactively labelled *pheA* (PH) and *nahH* (C23O) gene probes, generated with PCR.

### Conjugal mating experiments

Precultures of donor and recipient cells were inoculated from frozen stocks and, in all cases, pregrown aerobically overnight in Luria–Bertani (LB) broth (2 mL). For solid medium conjugation, approximately the same number of donor and recipient cells from mid-log phase ( $OD_{580\text{ nm}}$

0.8–1.0) were mixed in a microcentrifuge tube and inoculated on LB agar. Plates were incubated at 30 °C for 20 h. After mating, the cells were removed from LB agar with 2 mL sterile saline (0.85% NaCl), harvested by centrifugation and washed twice with sterile saline. The cells were resuspended in 1 mL of 0.85% NaCl. Serial dilutions were prepared and the number of prototrophic donor cells was determined by plating on MM supplemented with phenol, salicylic acid or glucose ( $2\text{ g L}^{-1}$ ), while auxotrophic donor cells were enumerated by plating on MM supplemented with phenol or salicylic acid, tryptophan ( $40\text{ g L}^{-1}$ ) and streptomycin ( $1000\text{ mg L}^{-1}$ ). Transconjugants of the auxotrophic strain were enumerated by plating on MM amended with phenol, salicylic acid, tryptophan and streptomycin while transconjugants of the prototrophic strain were enumerated by plating on MM supplemented with phenol and salicylic acid. The colonies of the transconjugants appeared usually after 2–7 days.

In triparental mating experiments, plasmid-mobilizing capacity for the PHE plasmid pEST1412 of *P. putida* PaW85 was tested with the helper strain *Escherichia coli* HB101 carrying pRK2013.

The conjugation frequency was calculated as the ratio of transconjugants ( $\text{CFU mL}^{-1}$ ) to donors ( $\text{CFU mL}^{-1}$ ) and the values are the mean of three independent experiments. No spontaneous streptomycin mutants of donor or recipient cells appeared on the selective media during the conjugations.

Plasmid profiles in donor and recipient strains after conjugational transfer were examined. The presence of plasmids in transconjugants was detected by the presence of the catabolic (*pheA* and *nahH*) and backbone (*repA* and *parA*) genes by PCR. The host strains of the putative transconjugants were confirmed by the REP-fingerprints with primer BOXA1R (Louws *et al.*, 1994). REP-PCR was carried out as described previously (Heinaru *et al.*, 2000).

**Table 2.** PCR primers used for amplification of DNA probes

Target/primers	Nucleotide sequence (5' → 3')	Temperature (°C)	Size (bp)	References
<i>pheA/pheA1</i>	CAGGATCGAATATCGGTGGCCTCG	60	947	Heinaru <i>et al.</i> (2000)
<i>pheA2</i>	CTTCACGCTGGCGTAACCAATCGC			
<i>nahH/ORF-F</i>	AGGTGWCGTSATGAAMAAAGG	60 → 50	934	Junca & Pieper (2003)
ORF-R	TYAGGTSAKMACGTTCAKGA			
IncP-9 <i>repA/rep9F</i>	CGCGGYACWTGGGTWCAGAC	58	447	This study
<i>rep9R</i>	GGYGGWTCATRCWGGRC			
pPHE20 <i>parA/parAF</i>	GAGCCTAGGAGTCTTGGGTG	57	952	This study
<i>parAR</i>	GAGAGCGAGAAGGTCTGTCG			
<i>carA/carA-F</i>	TTCAACACCGCCATGACCGG	55	617	Hilario <i>et al.</i> (2004)
<i>carA-R</i>	TGATGRCCSAGGCAGATRC			
BOXA1R	CTACGGCAAGCGACGCTGACG	53	Various	Louws <i>et al.</i> (1994)

## DNA sequencing and analysis

Nucleotide sequencing was carried out on a 3730xl DNA Analyzer (Applied Biosystems) using the BigDye<sup>®</sup> Terminator v3.1 Cycle Sequencing Kit (Applied Biosystems) and the protocols provided by the manufacturer. The pNAH20 nucleotide sequences obtained were aligned with the complete nucleotide sequence of pDTG1 and assembled according to this alignment, using BIOEDIT version 7.0.5.3 (Hall, 1999). Virtual restriction patterns were generated with the program PDRAW32 version 1.0 (<http://www.acaclone.com>). The *carA* phylogenetic tree was generated using the program CLUSTALX version 1.8 (Thompson et al., 2002). The complete nucleotide sequence of pNAH20 has been deposited in GenBank under the accession number AY887963. The nucleotide sequence of the 4259-bp HindIII fragment of the plasmid pNS8 has been deposited in GenBank under the accession number FJ975771. The nucleotide sequences of the *carA* genes of the strains 8R2ACX and NS8 have been deposited in GenBank under accession numbers FJ975772 and FJ975770, respectively.

## Enzyme assays

Induction experiments were performed with the strains *P. fluorescens* PC20 (pNAH20 and pPHE20) and *P. putida* NCIB 9816-4 (pDTG1) and G7 (NAH7) in 250-mL Erlenmeyer flasks containing 50 mL of MM supplemented with 0.2% (w/v) Casamino acids (CAA) and an inducing carbon source, phenol (2.5 mM) or salicylic acid (5 mM). In the induction experiments, fresh medium was inoculated with 5 mL of late exponential phase culture grown on the same medium without the inducer (in all cases, after inoculation, the OD<sub>580 nm</sub> of the culture was approximately 0.15). The induction of C23O, C12O and phenol monooxygenase (PMO) was studied in crude extracts of cells collected 4 h after the induction. Noninduced enzyme levels were determined in extracts from cells without the inducer. Crude extracts were prepared and all enzyme activity assays were performed as described previously (Heinaru et al., 2000). All experiments were run in triplicate.

## Growth kinetics

The growth of the strains was measured spectrophotometrically at 580 nm after every 30 min. All experiments were run in triplicate. The specific growth rate ( $\mu$ ) of the strain PC20 grown on phenol (2.5 mM), salicylic acid (2.5 mM) and their mixture (1.25 mM phenol+1.25 mM salicylic acid) was calculated from exponential growth phase of semi-logarithmic absorbance growth curves using the following equation:

$$\mu = \ln 2/t_d$$

where  $t_d$  is doubling time.

## Results

### Degradation of phenol and naphthalene by the strain PC20

*Pseudomonas fluorescens* PC20 has the ability to grow on phenol, salicylic acid and naphthalene. This strain expressed both C12O and C23O activity. Phenol was catabolized by the products of the inducible *pheBA* operon (C12O and PMO, respectively; Fig. 1). The catabolism of naphthalene was determined by the products of the *nah* genes, whereas the product of the *nahH* gene, C23O, was expressed constitutively (Fig. 1). When PC20 was grown on the mixture of phenol and salicylic acid, the consumption of both substrates occurred simultaneously despite the fact that two alternative degradative pathways were used. Similar values (about 0.35 h<sup>-1</sup>) were calculated for specific growth rate on phenol, salicylic acid and on the mixture of these substrates.

### Plasmid profile of the strain PC20

We have previously shown that the strain PC20 possesses C23O gene related to NahH gene of *P. putida* strains NCIB 9816-4 and G7 (Merimaa et al., 2006). Agarose gel electrophoresis of crude preparations of plasmid DNA showed that the strain PC20 harboured two large plasmids (Fig. 2). Southern blots of these two plasmids were hybridized against radioactively labelled DNA probes of NAH7-derived *nahH* (C23O) and *P. putida* pEST1412-derived *pheA* (PH) gene. The larger plasmid (pNAH20) revealed a strong hybridization signal with *nahH* gene probe and the smaller (pPHE20) hybridized with *pheA* gene (Fig. 2).

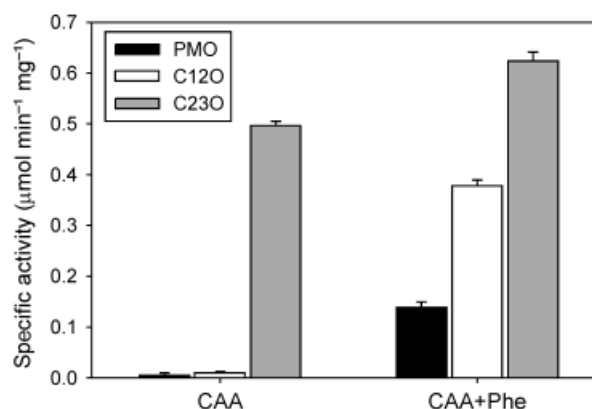


**Fig. 1.** Activities of catabolic enzymes (PMO, C12O and C23O) in noninduced or phenol-induced cells of the strain PC20. Values are means of at least three independently performed experiments.

### The complete nucleotide sequence of the plasmid pNAH20

Our preliminary sequencing results showed that the PC20 catabolic genes *nahR*, *nahG*, *nahT* and *nahH* were 100% identical to those of the IncP-9 naphthalene plasmid pDTG1 from *P. putida* NCIB 9816-4 (Dennis & Zylstra, 2004). Considering also the fact that the sizes of these two plasmids were similar, we performed comparative restriction analysis with EcoRI and HindIII (data not shown). We revealed that the restriction patterns of the two plasmids were almost

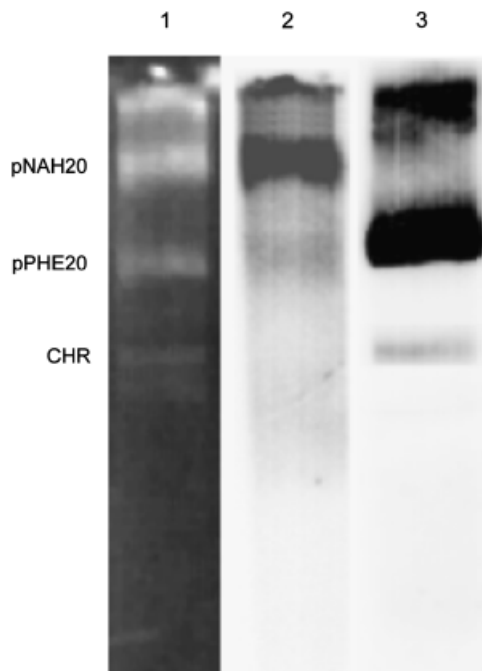


**Fig. 2.** Plasmid profile of the strain PC20 (lane 1) and its Southern hybridization probed with *nahH* of NAH7 (lane 2) and *pheA* of pEST1412 (lane 3). CHR, chromosomal DNA. A 0.8% agarose concentration was used in gel electrophoresis.

identical. Consequently, we designed a set of primers specific to pDTG1, covering the whole plasmid so that the resulting PCR products would be partially overlapping with each of its neighbour. The nucleotide sequences of the respective PCR products with pNAH20 as the template were aligned with the complete nucleotide sequence of pDTG1. The complete nucleotide sequence of pNAH20 was manually assembled according to these alignments. The virtual restriction pattern of the sequence obtained with EcoRI and HindIII was identical to the real one.

The plasmid pNAH20 is 83 042 bp in size and its nucleotide sequence is identical to pDTG1 (also 83 042 bp) except for two differences, the latter of which leads to the minor differences in the respective restriction patterns detected by us. First, there is a 1-bp mismatch – in position 22 078 of pNAH20, there is C instead of G in pDTG1; however, this mismatch also results in an altered amino acid sequence – the amino acid 181 of pNAH20 NahQ is Thr instead of Ser in pDTG1. Second and the most striking difference concerns the position and nucleotide sequence of insertion sequences. Namely, in pDTG1, between *nahT* and *nahG*, there is an insertion sequence (IS) element (1196 bp in size) that is 99% identical to IS*Pre1* of pCAR1 (Maeda *et al.*, 2003) (Fig. 3), while in pNAH20, this sequence is missing. Instead, pNAH20 has an IS element (positions 81 487–82 283) of exactly the same size, missing in pDTG1 between the positions 82 682 and 82 683, i.e. at the very end of the ORF of *orf93* (in pDTG1 designated as *orf826*), just upstream of the *mpf* mating pair formation genes, whose products are putatively involved in the synthesis of the conjugative pilus (Fig. 3). The IS element present in pNAH20 is 99% identical to IS*Pre2* of pCAR1 and 85% identical to the IS*Pre1*-like element in pDTG1 between *nahT* and *nahG*. Also, the two IS sequences are in reverse positions in these two plasmids with regard to the rest of the plasmid.

According to sequence similarities with the well-studied IncP-9 plasmid pWW0, *orf93/826* could be the first gene of the *mpf* operon, *mpfR*, encoding the transcriptional

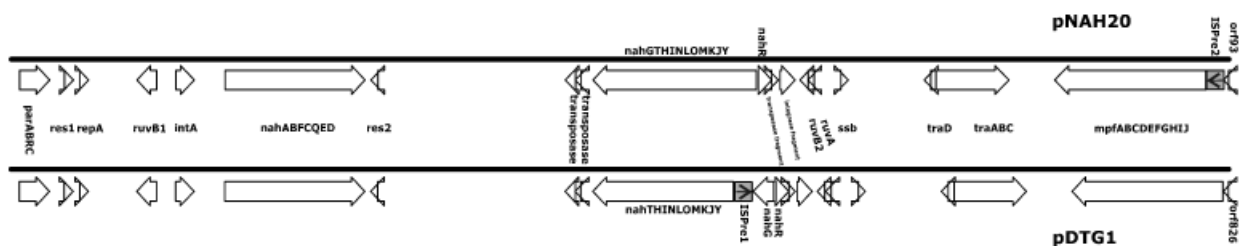


**Fig. 3.** Graphical alignment of the physical maps of the plasmids pNAH20 and pDTG1. The bold lines represent physical genome coordinates from base pairs 1 to 83 042 of both plasmids. The predicted genes/operons/ORFs of both plasmids are designated as arrows indicating direction of their transcription. The names of genes/operons/ORFs identical in two plasmids are given between the two graphical maps; differently designated regions are given below or above the respective plasmid. The IS*Pre1*- and IS*Pre2*-like elements in pDTG1 and pNAH20, respectively, are given as the grey boxes. The arrows inside the boxes show the direction of the transposase gene.

repressor of this operon (Greated *et al.*, 2002; Lambertsen *et al.*, 2004). As a result of the insertion of the ISPre2-like element, the very end of the predicted amino acid sequence of pNAH20 MpfR is substantially different from its counterparts coded by the other IncP-9 plasmids.

The discovered differences between pNAH20 and pDTG1 concerning the IS elements should affect expression/functioning of the genes near the insertion site, and thus the respective phenotypes of the two host strains – i.e. naphthalene/salicylate degradation functions coded by the lower operon of naphthalene degradation, *nahGTHINLQMKJY*, and conjugal transfer functions coded by the *mpf* genes. For this reason, we studied the expression of the *nahH* gene and the conjugation/mobilization functions of three IncP-9 NAH plasmids – pNAH20, pDTG1 and NAH7.

### Expression of the *nahH* gene of pNAH20, pDTG1 and NAH7

We studied catalytic activities of the key enzymes of both *meta*- and *ortho*-degradation pathways – the aromatic ring cleavage enzymes C23O and C12O, respectively, of the strains PC20, NCIB 9816-4 and G7 (Fig. 4). Induction of the *ortho*-cleavage pathway was detected during the growth of the strain PC20 on phenol, but not on salicylate; in case of NCIB 9816-4, salicylate, but not phenol, induced the activity of C12O. No C12O activity was detected in case of G7. The C23O activity was constitutively high in CAA-grown (non-induced) cells of PC20 and NCIB 9816-4. The induction with salicylic acid resulted in high C23O activity in strains PC20 and G7 (however, in PC20, the increase was only 2.3-fold compared with the 58-fold increase in case of G7) and negligible C23O activity in NCIB 9816-4. Interestingly, in the latter strain, the induced level on C23O activity was even six times lower than the basal level.

### Mating experiments using pNAH20, NAH7 and pDTG1 as helper plasmids

To investigate whether the plasmids pNAH20 and pPHE20 are conjugative/mobilizable, mating experiments were carried out. The results of these experiments, together with transfer frequencies, are given in Table 3. In all cases, the presence of plasmids in transconjugants was confirmed by PCR (Table 4) and gel electrophoresis of isolated plasmids (data not shown). Using the strain PC20 as the donor and *P. putida* PaW340 as the recipient, conjugation frequencies were typically  $10^{-3}$  and  $10^{-5}$  per donor for pNAH20 and pPHE20, respectively. Further transfer of pNAH20 and pPHE20 from PaW340 to prototrophic *P. putida* PaW85 succeeded only in case of pNAH20. Interestingly, from PaW340 (pNAH20 and pPHE20) [obtained from the mating experiments with PaW85 (pNAH20) as the donor and PaW340 (pPHE20) as the recipient], both plasmids trans-

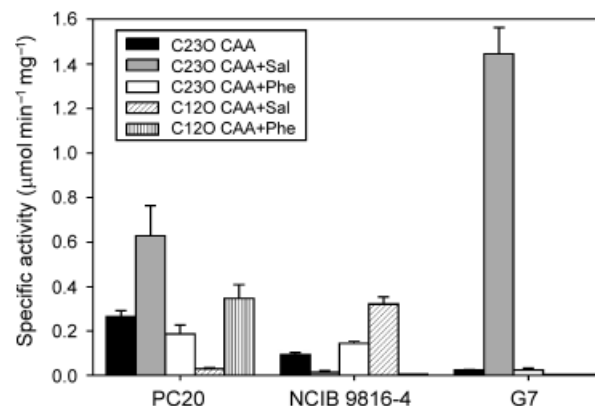


Fig. 4. Activities of C23O and C12O in noninduced or phenol- and salicylate-induced cells of the strains PC20, NCIB 9816-4 and G7. Values are means of at least three independently performed experiments.

ferred to PaW85 at the same frequency as from PC20 to PaW340 ( $10^{-4}$  and  $10^{-5}$ , respectively).

In order to study whether the IncP-9 NAH plasmids NAH7 and pDTG1 have the same pPHE20-mobilizing capabilities, we transferred these plasmids from G7 and NCIB 9816-4, respectively, to PaW340 (pPHE20). It is remarkable that the mating experiments using PaW340 (NAH7 and pPHE20) as the donor and PaW85 as the recipient resulted in no transconjugants containing only the plasmid pPHE20 (at frequencies  $< 10^{-8}$ ). We found transconjugants harbouring either only NAH7 or both plasmids pPHE20 and NAH7 at a transfer frequency approximately  $10^{-4}$  per donor.

In order to exclude the involvement of homologous recombination in the transfer of Nah<sup>+</sup> and Phe<sup>+</sup> phenotypes to recipient strains, matings with PaW340 (pNAH20 and pPHE20) and PaW340 (NAH7 and pPHE20) as donors and the *recA*-deficient derivative of PaW85 as the recipient were performed. As expected, the transfer frequencies were in the same range as in the cases using wt PaW85 cells as the recipient.

The mating experiments using PaW340 (pDTG1 and pPHE20) as the donor and PaW85 as the recipient showed that both plasmids were transferred at frequencies two orders of magnitude lower than in case of PC20 or PaW340 (pNAH20 and pPHE20) as the donor ( $10^{-5}$  and  $10^{-7}$ , respectively).

### pNAH20 conjugates and mobilizes pPHE20 into the indigenous plasmid-free *P. fluorescens* isolate 8R2ACX

The strain 8R2ACX (not able to grow on phenol, salicylic acid and naphthalene, does not harbour any plasmids) was used as the recipient strain in mating experiments.

**Table 3.** Donors, recipients, transconjugants and transfer frequencies in mating experiments

Donor strain and plasmid	Recipient strain	Transconjugant	Transfer frequency
PC20 (pNAH20, pPHE20)	PaW340	PaW340 (pNAH20)	$2.55 (\pm 0.95) \times 10^{-3}$
		PaW340 (pPHE20)	$4.95 (\pm 2.13) \times 10^{-5}$
PaW340 (pNAH20)	PaW85	PaW85 (pNAH20)	$3.07 (\pm 1.10) \times 10^{-4}$
PaW340 (pPHE20)	PaW85	No transfer	
PaW85 (pNAH20)	PaW340 (pPHE20)	PaW340 (pNAH20, pPHE20)	ND
PaW340 (pNAH20, pPHE20)	PaW85	PaW85 (pNAH20)	$1.94 (\pm 0.53) \times 10^{-4}$
		PaW85 (pPHE20)	$1.27 (\pm 0.09) \times 10^{-5}$
PaW340 (pNAH20, pPHE20)	PaW85 <i>recA</i> <sup>-</sup>	PaW85 <i>recA</i> <sup>-</sup> (pNAH20)	$1.66 (\pm 0.14) \times 10^{-5}$
		PaW85 <i>recA</i> <sup>-</sup> (pPHE20)	$1.09 (\pm 0.12) \times 10^{-6}$
G7 (NAH7)	PaW340 (pPHE20)	PaW340 (NAH7, pPHE20)	ND
PaW340 (NAH7, pPHE20)	PaW85	PaW85 (NAH7, pPHE20)	$4.25 (\pm 0.67) \times 10^{-4}$
PaW340 (NAH7, pPHE20)	PaW85 <i>recA</i> <sup>-</sup>	PaW85 <i>recA</i> <sup>-</sup> (NAH7, pPHE20)	$2.02 (\pm 0.11) \times 10^{-4}$
NCIB 9816-4 (pDTG1)	PaW340 (pPHE20)	PaW340 (pDTG1, pPHE20)	ND
PaW340 (pDTG1, pPHE20)	PaW85	PaW85 (pDTG1)	$9.7 (\pm 0.5) \times 10^{-6}$
		PaW85 (pPHE20)	$2.59 (\pm 1.26) \times 10^{-7}$
PaW340 (pNAH20, pPHE20)	8R2ACX	8R2ACX (pNAH20)	$9 \times 10^{-7}$
		8R2ACX (pPHE20)	$3.7 \times 10^{-8}$
PaW85 (pEST1412)	PaW340	No transfer	
PaW85 (pEST1412) × HB101 (pRK2013)	PaW340	PaW340 (pEST1412)	ND
PaW85 (pNAH20)	PaW340 (pEST1412)	PaW340 (pNAH20, pEST1412)	$4.7 \times 10^{-5}$
PaW340 (pNAH20, pEST1412)	PaW85	PaW85 (pNAH20)	$7.5 \times 10^{-4}$
		PaW85 (pEST1412)	ND
NS8 (pNS8)	PaW340	No transfer	

ND, not determined.

**Table 4.** Characteristics of the transconjugants

Transconjugant	C23O gene-PCR	<i>pheA</i> gene-PCR	IncP-9 <i>repA</i> gene PCR	pPHE20 <i>parA</i> gene PCR	REP-PCR profile*
PaW340 (pNAH20)	+	-	+	-	a
PaW340 (pPHE20)	-	+	-	+	a
PaW85 (pNAH20)	+	-	+	-	a
PaW340 (pNAH20, pPHE20)	+	+	+	+	a
PaW85 (pPHE20)	-	+	-	+	a
PaW340 (NAH7, pPHE20)	+	+	+	+	a
PaW85 (NAH7, pPHE20)	+	+	+	+	a
PaW340 (pDTG1, pPHE20)	+	+	+	+	a
PaW85 (pDTG1)	+	-	+	-	a
8R2ACX (pNAH20)	+	-	+	-	b
8R2ACX (pPHE20)	-	+	-	+	b
PaW340 (pEST1412)	-	+	-	+	a
PaW340 (pNAH20, pEST1412)	+	+	+	+	a

+, positive reaction; -, negative reaction.

\*REP-PCR profile was obtained using BOXA1R primer: a, *Pseudomonas putida* PaW340 or PaW85; b, *Pseudomonas fluorescens* 8R2ACX.

Transconjugants were selected and confirmed (Table 4) as mentioned above. The comparison of the 16S rRNA and *carA* genes (the latter encodes the small subunit of carbamoylphosphate synthase) of strains PC20 and 8R2ACX showed 100% and 92% identities, respectively, which allowed us to classify this strain also as *P. fluorescens*. The transfer of pNAH20 and pPHE20 from PaW340 (pNAH20 and pPHE20) to the indigenous

8R2ACX strain was monitored. In this case, the transfer frequencies were approximately three orders of magnitude lower than the frequencies for pNAH20 and pPHE20 in conjugation from the same donor strain to PaW85 (Table 3). The strain 8R2ACX produces exopolysaccharides that can function as a physical barrier against the transfer process and cause the observed reduction in transfer frequencies.

### The helper function of pNAH20 in the transfer of the PHE plasmid pEST1412 into *P. putida* PaW85

We studied whether the nonconjugative PHE plasmid pEST1412 can be transferred by the helper plasmid pNAH20. The plasmid pEST1412 was successfully used in bioaugmentation application 20 years ago (Peters *et al.*, 1997) and it consists of the *pheBA* operon cloned into the vector plasmid pAYC32 having RSF1010 replicon (Kivisaar *et al.*, 1990). We first performed triparental mating with PaW85 (pEST1412) as the donor, *E. coli* HB101 containing pRK2013 (IncP-1 transfer genes inserted into ColE1 replicon) as the helper and PaW340 as the recipient (Table 3). The achieved transconjugant PaW340 (pEST1412) was then used as a recipient, and PaW85 (pNAH20) as a donor, resulting in PaW340 containing both plasmids pNAH20 and pEST1412, a suitable strain to examine mobilization of pEST1412 by pNAH20 into PaW85. Indeed, both transconjugants PaW85 (pNAH20) and PaW85 (pEST1412) were obtained.

### In situ transfer of the NAH plasmid pNAH20

*Pseudomonas fluorescens* PC20 was used among other strains in bioaugmentation experiments carried out in the phyto-remediation test plots in the semi-coke (oil shale chemical industry solid waste) depository (Truu *et al.*, 2003; Juhanson *et al.*, 2009). Birch trees were planted into semi-coke in 1998. Biomass of PC20 and other strains was supplied to some parts of these test plots (each 10 m<sup>2</sup>) in June 2006. Each treatment received approximately 5 L of the bacterial suspension of PC20 with a concentration of 10<sup>8</sup> CFU mL<sup>-1</sup>. In October 2007, we isolated a salicylate-degrading *P. fluorescens* strain NS8 from the birch rhizosphere of one of these plots, which, according to REP-fingerprint, was not PC20 (Fig. 7). This strain contained one large plasmid named pNS8, whose HindIII restriction pattern was identical to the one of pNAH20 (data not shown) with one exception – instead of a 3065-bp fragment, we detected a band with the size approximately 4200 bp, not present among pNAH20 restriction fragments. The respective region was analysed by PCR and sequencing, and it turned out that between the positions 81 244 and 81 245, i.e. in the middle of the *mpfA* gene, 242 bp apart from the other ISPre2-like sequence, another ISPre2-like sequence was inserted (Fig. 5). This sequence is 100% identical to the IS element at the end of the ORF of *orf93* (*mpfR*), but in reverse direction. Comparison of virtual and real HindIII restriction analyses (data not shown) proved that beside this insertion, the rest of the sequence of pNS8 should be identical to the one of pNAH20.

We also compared the HindIII restriction patterns of the transconjugant strains PaW340 (pNAH20) and PaW85 (pNAH20) in order to detect possible changes in the structure of pNAH20 during transfer under laboratory

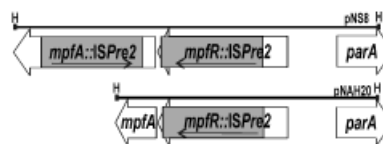


**Fig. 5.** Graphical alignment of HindIII restriction fragments (bold lines with letters H at the ends) of the plasmids pNS8 (upper, 4259 bp) and pNAH20 (lower, 3065 bp). The arrows indicate the respective genes with the direction of transcription. The ISPre2-like elements are given as the grey boxes. The arrows inside the boxes show the direction of transposase gene.

conditions. The sizes of all restriction fragments of these two plasmids were identical (data not shown).

The product of the *mpfA* gene is a homologue of the VirB2 protein of type-IV secretion system of *Agrobacterium tumefaciens*, which has been shown to be a major pilus protein (Backert *et al.*, 2008). Insertion of 1196 bp in the middle of the *mpfA* gene of pNS8 most likely disrupts the structure of MpfA, and the correct pilus could not be formed. Indeed, the transfer experiments using NS8 as the donor and PaW340 as the recipient resulted in no transconjugants (Table 3).

### Phylogenetic analysis of the indigenous *P. fluorescens* strains PC20, 8R2ACX and NS8

As the sequences of 16S rRNA genes of the indigenous *P. fluorescens* strains PC20, 8R2ACX and NS8 are 100% identical, we performed phylogenetic analysis of these three strains using the *carA* gene. As reference strains, we used representatives of different *P. fluorescens* biotypes and one strain belonging to another species of the genus *Pseudomonas*, namely *Pseudomonas mendocina*. According to the phylogenetic tree obtained (Fig. 6), the strains 8R2ACX and NS8 are very close to each other and form a separate cluster with their closest relative PC20. Thus, the strains 8R2ACX and NS8 belong to the same biotype F of *P. fluorescens* as PC20.

As the *carA* sequences of 8R2ACX and NS8 are extremely close to each other, we performed REP-fingerprinting of these two strains. As shown in Fig. 7, it turned out that 8R2ACX was the same strain as NS8, but without any plasmids.

### Discussion

Self-transmissible broad-host-range catabolic plasmids play a crucial role in dissemination of catabolic functions in polluted areas (Dennis, 2005; Thomas & Nielsen, 2005). The mobilizing capacity of these plasmids even broadens their impact on HGT (Francia *et al.*, 2004). In this study, we describe the *P. fluorescens* strain PC20 that harbours two large plasmids – pNAH20 and pPHE20. Our conjugation



**Fig. 6.** Bootstrapped neighbour-joining tree derived from multiple alignment of the *carA* genes of the newly isolated strains 8R2ACX and NS8 (in boldface) together with different *Pseudomonas* strains, constructed with the CLUSTALX program. The GenBank accession numbers of the reference sequences are indicated in parentheses. The numbers at the nodes of the trees represent the bootstrap values (1000 replicates) for each node.

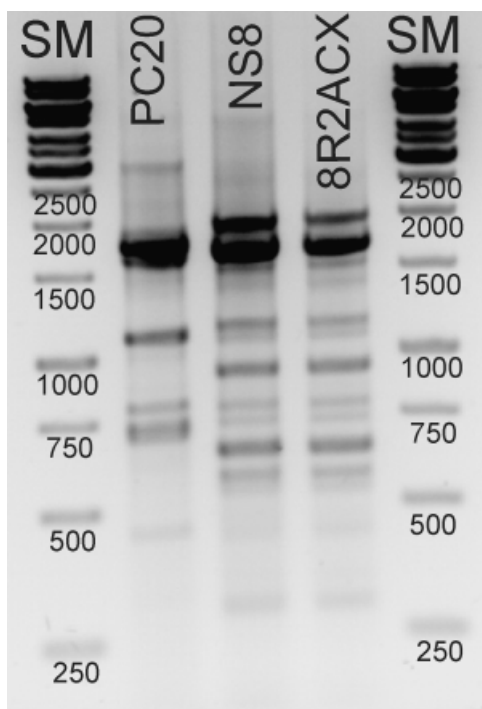
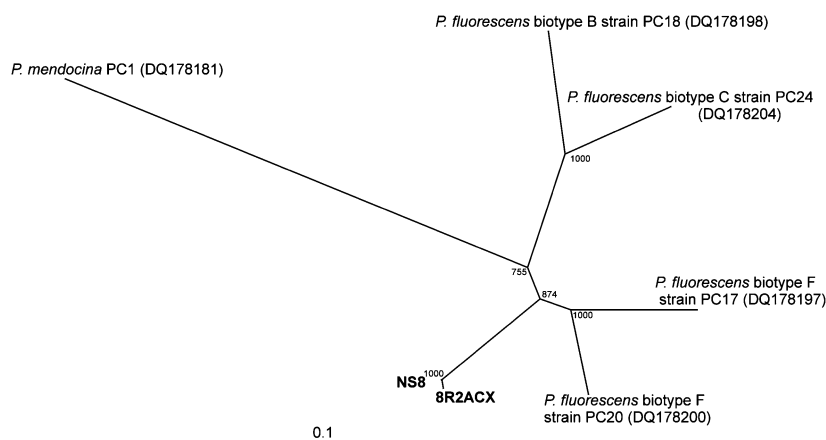


**Fig. 7.** REP-fingerprints of the strains PC20, NS8 and 8R2ACX. Sizes (bp) of the fragments of the DNA size marker (SM, GeneRuler™ 1-kb DNA Ladder, Fermentas) are shown. A 1.5% agarose concentration was used in gel electrophoresis.

experiments showed that pNAH20 is self-transmissible, while pPHE20 is mobilizable by pNAH20.

These plasmids enable the host strain to degrade naphthalene and phenol simultaneously via catechol *meta* and *ortho* degradation pathways, respectively. Possessing two alternative catechol degradation pathways and constitutively synthesized C23O could provide an advantage in the degradation of different aromatic substrates under natural condi-

tions, thus favouring the stable coexistence of these two large catabolic plasmids.

The complete nucleotide sequence of the broad-host-range IncP-9 plasmid pNAH20 shows that this plasmid is almost identical to another fully sequenced NAH plasmid pDTG1 (Dennis & Zylstra, 2004). Many studies have reported that plasmids with identical molecular structures have been isolated from different geographic locations. The host strain of the plasmid pDTG1, *P. putida* NCIB 9816-4, was isolated in Wales (Serdar & Gibson, 1989). Our identification of pNAH20 in *P. fluorescens* PC20, isolated in Estonia, supports the suggestion that pDTG1-like plasmids are disseminated around the world and might have played an important role in the adaptation of microbial communities to various oil-contaminated sites (Ono *et al.*, 2007; Sevastysyanovich *et al.*, 2008).

Despite the striking similarity in size and nucleotide sequence of pDTG1 and pNAH20, the position of IS elements significantly alters the functions provided by the two plasmids. It has been shown that in the strain NCIB 9816-4 harbouring pDTG1 the plasmid-encoded lower operon of naphthalene degradation is inoperative due to the insertion of the IS*Pre1*-like element between the first and the second gene of the operon (Dennis & Zylstra, 2004). The presence of the IS element produces a stem-loop structure preventing the expression of the downstream genes. For complete naphthalene degradation, this strain utilizes the chromosomally encoded *ortho*-cleavage pathway instead of the defective pDTG1-encoded *meta*-cleavage route. In NAH7 and pNAH20, there is no IS element disrupting the lower naphthalene operon. Our studies of the catalytic activities of the key enzymes of both *meta*- and *ortho*-degradation pathways of the strains PC20, NCIB 9816-4 and G7 provide a solid proof that NCIB 9816-4 uses the catechol *ortho*-cleavage pathway for growth on naphthalene, while in PC20 and G7, the plasmid-encoded *meta*-pathway

is sufficient for complete degradation of naphthalene. Although the strain PC20 effectively degrades naphthalene, the reason why this substrate is not degraded by the pDTG1-encoded catechol *meta* pathway in NCIB 9816-4 might be the low inducibility of the *nahH* gene coding for C23O as compared with NAH7-encoded C23O.

In case of pNAH20, vice versa, insertion of the ISPre2-like element increases the transfer frequency of pNAH20 about 100-fold as compared with pDTG1 probably due to elevation of the expression level of the *mpf* genes. In case of pNS8 (the derivative of pNAH20 isolated from the birch rhizosphere transconjugant *P. fluorescens* NS8 after bioaugmentation experiment), insertion of the second copy of ISPre2 abolishes the transfer function of this plasmid. Insertion of ISPre2-like elements into pNAH20 and pNS8 were carried out into ORFs of the *mpfR* and *mpfA* genes, respectively, leading to altered amino acid sequences. At least in case of MpfA, the major pilus protein, insertion disrupts the structure of this protein, and as the correct pilus could not be formed in this strain, pNS8 is not able to self-transfer. The natural pNAH20 transconjugant strain NS8 probably did not tolerate the high metabolic load caused by the elevated expression level of the *mpf* genes. It has been shown in case of all studied large conjugative plasmids that their transfer systems encode regulatory circuits that help to minimize this burden (Zatyka & Thomas, 1998).

Different direction of these IS elements also seems to play a role in this different outcome probably by producing DNA secondary structures or providing promoter regions preventing or increasing the expression of the downstream genes, respectively, thus inactivating or activating the whole/most of the operon. In case of pNAH20, the elevation of the expression of the *mpf* genes may be caused by reduction of MpfR repressor function and/or a promoter sequence provided by the ISPre2-like element. Thus, the host strain can modulate the plasmid (backbone) functions to fit its own needs. This reflects the plasticity of plasmid genomes and is possibly an indication how bacteria quickly adapt to different needs through genetic rearrangements.

The strain PC20 is an effective degrader of pollutants; it persists under natural conditions quite long (Juhanson *et al.*, 2009), and tolerates the high transfer/mobilization activity of pNAH20. Although NAH7 and pDTG1 can also mobilize pPHE20, pNAH20 is much more efficient in this function. Additionally, pNAH20 also mobilizes the IncQ broad-host-range plasmid RSF1010-based PHE plasmid pEST1412. Thus, this strain and this plasmid (backbone) can be used as a successful tool for bioremediation.

We studied the transfer of pNAH20 and pPHE20 only in birch rhizosphere because this environment supports dense bacterial communities and has been classified as a hot spot for HGT (Lilley *et al.*, 1994; Musovic *et al.*, 2006). In case of plasmids coding for rigid and short mating pili (e.g. IncP

plasmids), the frequency of transmission by conjugation is generally higher on solid surfaces than in liquids (Sayler *et al.*, 1990). Indeed, our rhizoremediation/bioaugmentation experiments yielded a natural transconjugant of pNAH20. During *in vitro* transfer experiments, we acquired transconjugants of both plasmids pNAH20 and pPHE20. Thus, it could be hypothesized that mobilization of the latter plasmid by the helper plasmid pNAH20 into the indigenous representative of the genus *Pseudomonas* might take place under natural conditions as well. Interestingly, we isolated the same *P. fluorescens* strain with (NS8) and without (8R2ACX) the pNAH20 derivative from the rhizosphere sample of the same bioaugmentation test plot. This strain is phylogenetically very close to PC20, which indicates that the optimal host for pNAH20 should be *P. fluorescens* biotype F. This is consistent with the notion that the plasmid NAH7 transfers conjugally to and remains in *Gammaproteobacteria* and not in *Alpha-* or *Betaproteobacteria* (Miyazaki *et al.*, 2008).

Our results demonstrate an excellent example of HGT under natural conditions. We show that plasmid mobilization might be a more important mechanism of HGT than expected. However, to understand more precisely the mechanism of mobilization of pPHE20 by pNAH20, we will undertake the complete nucleotide sequencing of the PHE plasmid of PC20.

## Acknowledgements

This study was supported by the Institute of Molecular and Cell Biology, Tartu University, by the Estonian Science Foundation Grant 7827, and Research Grant SF0180026s08 from the Estonian Ministry of Education and Research.

## Authors' contribution

E.H. and E.V. contributed equally to this paper.

## References

- Backert S, Fronzes R & Waksman G (2008) VirB2 and VirB5 proteins: specialized adhesins in bacterial type-IV secretion systems? *Trends Microbiol* **16**: 409–413.
- Bayley SA, Duggleby CJ, Worsey MJ, Williams PA, Hardy KG & Broda P (1977) Two modes of loss of the Tol function from *Pseudomonas putida* mt-2. *Mol Gen Genet* **154**: 203–204.
- Boyer HW & Roulland-Dussoix D (1969) A complementation analysis of the restriction and modification of DNA in *Escherichia coli*. *J Mol Biol* **41**: 459–472.
- Cerniglia C (1992) Biodegradation of polycyclic aromatic hydrocarbons. *Biodegradation* **3**: 351–368.
- Connors MA & Barnsley EA (1982) Naphthalene plasmids in pseudomonads. *J Bacteriol* **149**: 1096–1101.

- Dennis JJ (2005) The evolution of IncP catabolic plasmids. *Curr Opin Biotechnol* **16**: 291–298.
- Dennis JJ & Zylstra GJ (2004) Complete sequence and genetic organization of pDTG1, the 83 kilobase naphthalene degradation plasmid from *Pseudomonas putida* strain NCIB 9816-4. *J Mol Biol* **341**: 753–768.
- Dunn NW & Gunsalus IC (1973) Transmissible plasmid coding early enzymes of naphthalene oxidation in *Pseudomonas putida*. *J Bacteriol* **114**: 974–979.
- Eaton RW & Chapman PJ (1992) Bacterial metabolism of naphthalene – construction and use of recombinant bacteria to study ring cleavage of 1,2-dihydroxynaphthalene and subsequent reactions. *J Bacteriol* **174**: 7542–7554.
- Figurski DH & Helinski DR (1979) Replication of an origin-containing derivative of plasmid RK2 dependent on a plasmid function provided in trans. *P Natl Acad Sci USA* **76**: 1648–1652.
- Francia MV, Varsaki A, Garcillan-Barcia MP, Latorre A, Drainas C & de la Cruz F (2004) A classification scheme for mobilization regions of bacterial plasmids. *FEMS Microbiol Rev* **28**: 79–100.
- Franklin FCH & Williams PA (1980) Construction of a partial diploid for the degradative pathway encoded by the TOL plasmid (pWW0) from *Pseudomonas putida* mt-2 – evidence for the positive nature of the regulation by the *xylR* gene. *Mol Gen Genet* **177**: 321–328.
- Greated A, Lambertsen L, Williams PA & Thomas CM (2002) Complete sequence of the IncP-9 TOL plasmid pWW0 from *Pseudomonas putida*. *Environ Microbiol* **4**: 856–871.
- Hall T (1999) BioEdit: a user-friendly biological sequence alignment editor and analysis program for Windows 95/98/NT. *Nucleic Acids Sym Ser* **41**: 95–98.
- Heinaru E, Truu J, Stottmeister U & Heinaru A (2000) Three types of phenol and *p*-cresol catabolism in phenol- and *p*-cresol-degrading bacteria isolated from river water continuously polluted with phenolic compounds. *FEMS Microbiol Ecol* **31**: 195–205.
- Heinaru E, Merimaa M, Viggor S, Lehiste M, Leito I, Truu J & Heinaru A (2005) Biodegradation efficiency of functionally important populations selected for bioaugmentation in phenol- and oil-polluted area. *FEMS Microbiol Ecol* **51**: 363–373.
- Heuer H, Abdo Z & Smalla K (2008) Patchy distribution of flexible genetic elements in bacterial populations mediates robustness to environmental uncertainty. *FEMS Microbiol Ecol* **65**: 361–371.
- Hilario E, Buckley TR & Young JM (2004) Improved resolution on the phylogenetic relationships among *Pseudomonas* by the combined analysis of *atpD*, *carA*, *recA* and 16S rDNA. *Antonie van Leeuwenhoek* **86**: 51–64.
- Juhanson J, Truu J, Heinaru E & Heinaru A (2009) Survival and catabolic performance of introduced bacterial strains during phytoremediation and bioaugmentation field experiment. *FEMS Microbiol Ecol*, DOI: 10/1111/j.1574-6941.2009.00754.x.
- Junca H & Pieper DH (2003) Amplified functional DNA restriction analysis to determine catechol 2,3-dioxygenase gene diversity in soil bacteria. *J Microbiol Meth* **55**: 697–708.
- Kivisaar M, Horak R, Kasak L, Heinaru A & Habicht J (1990) Selection of independent plasmids determining phenol degradation in *Pseudomonas putida* and the cloning and expression of genes encoding phenol monooxygenase and catechol 1,2-dioxygenase. *Plasmid* **24**: 25–36.
- Kivisaar MA, Habicht JK & Heinaru AL (1989) Degradation of phenol and *m*-toluate in *Pseudomonas* sp. strain EST1001 and its *Pseudomonas putida* transconjugants is determined by a multiplasmid system. *J Bacteriol* **171**: 5111–5116.
- Lambertsen LM, Molin S, Kroer N & Thomas CM (2004) Transcriptional regulation of pWW0 transfer genes in *Pseudomonas putida* KT2440. *Plasmid* **52**: 169–181.
- Li W, Shi J, Wang X *et al.* (2004) Complete nucleotide sequence and organization of the naphthalene catabolic plasmid pND6-1 from *Pseudomonas* sp. strain ND6. *Gene* **336**: 231–240.
- Lilley AK, Fry JC, Day MJ & Bailey MJ (1994) *In situ* transfer of an exogenously isolated plasmid between *Pseudomonas* spp. in sugar-beet rhizosphere. *Microbiology* **140**: 27–33.
- Llosa M & de la Cruz F (2005) Bacterial conjugation: a potential tool for genomic engineering. *Res Microbiol* **156**: 1–6.
- Louws FJ, Fulbright DW, Stephens CT & de Bruijn FJ (1994) Specific genomic fingerprints of phytopathogenic *Xanthomonas* and *Pseudomonas* pathovars and strains generated with repetitive sequences and PCR. *Appl Environ Microb* **60**: 2286–2295.
- Maeda K, Nojiri H, Shintani M, Yoshida T, Habe H & Omori T (2003) Complete nucleotide sequence of carbazole/dioxin-degrading plasmid pCAR1 in *Pseudomonas resinovorans* strain CA10 indicates its mosaicity and the presence of large catabolic transposon Tn4676. *J Mol Biol* **326**: 21–33.
- Merimaa M, Heinaru E, Liivak M, Vedler E & Heinaru A (2006) Grouping of phenol hydroxylase and catechol 2,3-dioxygenase genes among phenol- and *p*-cresol-degrading *Pseudomonas* species and biotypes. *Arch Microbiol* **186**: 287–296.
- Miyazaki R, Ohtsubo Y, Nagata Y & Tsuda M (2008) Characterization of the *traD* operon of naphthalene-catabolic plasmid NAH7: a host-range modifier in conjugative transfer. *J Bacteriol* **190**: 6281–6289.
- Musovic S, Oregaard G, Kroer N & Sorensen SJ (2006) Cultivation-independent examination of horizontal transfer and host range of an IncP-1 plasmid among gram-positive and gram-negative bacteria indigenous to the barley rhizosphere. *Appl Environ Microb* **72**: 6687–6692.
- Ono A, Miyazaki R, Sota M, Ohtsubo Y, Nagata Y & Tsuda M (2007) Isolation and characterization of naphthalene-catabolic genes and plasmids from oil-contaminated soil by using two cultivation-independent approaches. *Appl Microbiol Biot* **74**: 501–510.
- Peters M, Heinaru E, Talpsep E, Wand H, Stottmeister U, Heinaru A & Nurk A (1997) Acquisition of a deliberately introduced

- phenol degradation operon, *pheBA*, by different indigenous *Pseudomonas* species. *Appl Environ Microb* **63**: 4899–4906.
- Romine MF, Stillwell LC, Wong KK *et al.* (1999) Complete sequence of a 184-kilobase catabolic plasmid from *Sphingomonas aromaticivorans* F199. *J Bacteriol* **181**: 1585–1602.
- Sambrook J, Fritsch EF & Maniatis T (1989) *Molecular Cloning: A Laboratory Manual*. Cold Spring Harbor Laboratory Press, Cold Spring Harbor, NY.
- Sayler GS, Hooper SW, Layton AC & King JMH (1990) Catabolic plasmids of environmental and ecological significance. *Microb Ecol* **19**: 1–20.
- Serdar CM & Gibson DT (1989) Isolation and characterization of altered plasmids in mutant strains of *Pseudomonas putida* NCIB-9816. *Biochem Biophys Res Commun* **164**: 764–771.
- Sevastyanovich YR, Krasowiak R, Bingle LE *et al.* (2008) Diversity of IncP-9 plasmids of *Pseudomonas*. *Microbiology* **154**: 2929–2941.
- Shingler V, Franklin FC, Tsuda M, Holroyd D & Bagdasarian M (1989) Molecular analysis of a plasmid-encoded phenol hydroxylase from *Pseudomonas* CF600. *J Gen Microbiol* **135**: 1083–1092.
- Sota M, Yano H, Ono A *et al.* (2006) Genomic and functional analysis of the IncP-9 naphthalene-catabolic plasmid NAH7 and its transposon Tn4655 suggests catabolic gene spread by a tyrosine recombinase. *J Bacteriol* **188**: 4057–4067.
- Stuart-Keil KG, Hohnstock AM, Drees KP, Herrick JB & Madsen EL (1998) Plasmids responsible for horizontal transfer of naphthalene catabolism genes between bacteria at a coal tar-contaminated site are homologous to pDTG1 from *Pseudomonas putida* NCIB 9816-4. *Appl Environ Microb* **64**: 3633–3640.
- Tegova R, Tover A, Tarassova K, Tark M & Kivisaar M (2004) Involvement of error-prone DNA polymerase IV in stationary-phase mutagenesis in *Pseudomonas putida*. *J Bacteriol* **186**: 2735–2744.
- Thomas CM & Nielsen KM (2005) Mechanisms of, and barriers to, horizontal gene transfer between bacteria. *Nat Rev Microbiol* **3**: 711–721.
- Thompson JD, Gibson TJ & Higgins DG (2002) Multiple sequence alignment using ClustalW and ClustalX. *Curr Protoc Bioinformatics*, chapter 2, Unit 2.3:1–22.
- Truu J, Talpsep E, Vedler E, Heinaru E & Heinaru A (2003) Enhanced biodegradation of oil shale chemical industry solid wastes by phytoremediation and bioaugmentation. *Oil Shale* **20**: 421–428.
- Zatyka M & Thomas CM (1998) Control of genes for conjugative transfer of plasmids and other mobile elements. *FEMS Microbiol Rev* **21**: 291–319.